IOP Publishing Journal of Physics: Condensed Matter
J. Phys.: Condens. Matter **32** (2020) 175302 (9pp) https://doi.org/10.1088/1361-648X/ab699f

The effects of strain and electric field on the half-metallicity of pristine and O–H/C–N-decorated zigzag graphene nanoribbons

Shidong Zhang[1], Can Cao[1], Bowen Zeng[1] and Mengqiu Long[1,2,3]

[1] Hunan Key laboratory of Super Micro-structure and Ultrafast Process, School of Physics and Electronics, Central South University, Changsha 410083, People's Republic of China
[2] Institute of Low-dimensional Quantum Materials and Devices, School of Physical Science and Technology, Xinjiang University, Urumqi, 830046, People's Republic of China

E-mail: mqlong@csu.edu.cn (M Long)

Received 18 October 2019, revised 11 December 2019
Accepted for publication 9 January 2020
Published 28 January 2020

Abstract

In zigzag graphene nanoribbons (ZGNRs), the spin polarized edge states play a significant role in the electronic structure. The two ferromagnetically ordered edges anti-ferromagnetically coupled with each other, which would result in the half-metallicity under electric field. Given that the strain, external electric field, and edge decorations are the main means of tuning the magnetism and electronic property of one-dimentional materials. It motivates us to study the combine effects on ZGNRs of these methods. So, in present work, the corporate influences of the tensile strain, transverse electric field, and asymmetric edge decoration by −OH and −CN groups on the magnetism and electronic property of 8-ZGNR have been studied using the density functional theory. The calculational results indicate that the arising strain can modulate the response of electronic and magnetic properties to external electric field, improving the magnetism and extending the electric field range in which the ZGNR presents half-metallicity. In addition, the O-H/C-N groups decorated ZGNR possesses a lower critic electric field and a larger electric field range for realizing half-metallicity comparing with the unstrained pristine ZGNR.

Keywords: zigzag graphene nanoribbon, strain, electric field, half-metallicity, spin polarization, edge decoration

(Some figures may appear in colour only in the online journal)

1. Introduction

As the first member of single-atom-thick two-dimensional (2D) material obtained in experiment [1], graphene draws numerous attentions of researchers and has been studied extensively due to the distinctive properties such as the perfect Dirac cone [2], obvious quantum Hall effect [3], excellent mechanical property [4], high carrier mobility [5] and thermal conductivity [6], and unique transport property [7]. Although many other 2D materials such as silicene [8], graphdiyne sheet [9–11], boron nitride sheet [12], layered transition-metal dichalcogenides (TMDs) [13–15], phosphorene [16], borophene [17], tellurene [18], and the planar metal-organic framework [19] gradually stepped into people's horizon, graphene remains one of the focuses of nano-materials and nano-electronics owing to the mature preparation method, and opportunities for functionalization, such as cutting [20, 21], doping [22, 23], stacking [24, 25], strain [26, 27], external field [28], and covalent decoration [29].

Owing to the spin polarized edge states, zigzag graphene nanoribbons (ZGNR) aroused much interest for the potential applications in spintronics. The unpaired electrons caused by the breaking C–C bond formed two subbands near the Fermi level (FL), which induce the high density of states (DOS) at

[3] Author to whom any correspondence should be addressed.

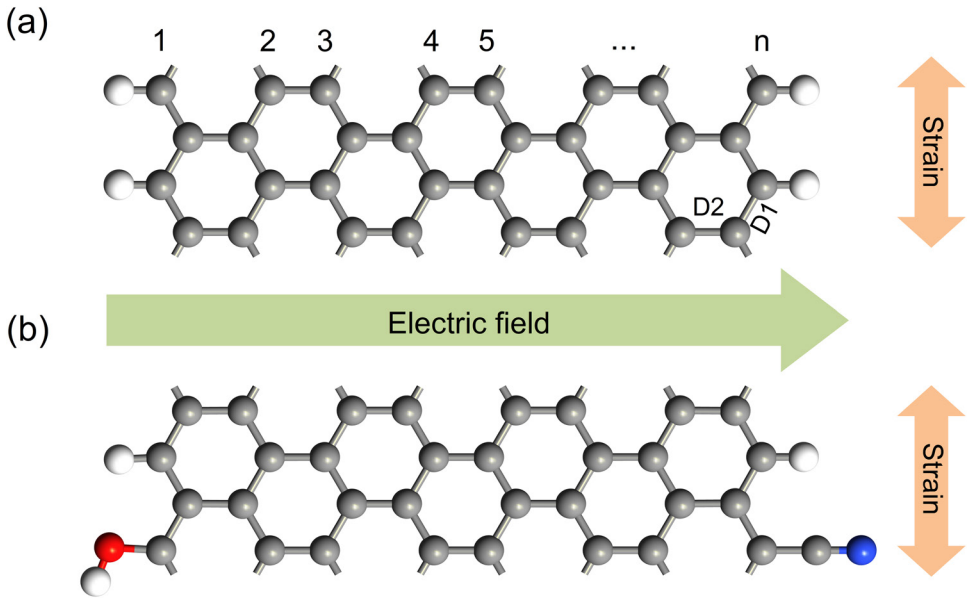

Figure 1. (a) The geometric structures of pristine ZGNR. (b) The geometric structures ZGNR that edge decorated by −OH and −CN groups. The gray, blue, red, and white balls represent the C, N, O, and H atoms, respectively. The pale green and yellow arrows show the directions of electric field and strain applied on ZGNR respectively. D1 and D2 denote the bond length of C–C located at the nearest edge and the next nearest edge, respectively.

the FL and lead to the metallicity of ZGNR [21, 30]. When the coulomb repulsion between electrons is taken into account, to lower the total energy, the system tends towards splitting the edge states, and then anti-ferromagnetically couples the opposite edges [30]. When a transverse electric field is applied in paralleling with the plane of ZGNR, the local edge states corresponding to the edge with high electrostatic potential are shifted downwards and the other edge with lower electrostatic potential are shifted upwards, leading to the half-metallicity [31]. Owing to the symmetry-dependent coupling between π and π^* subbands, the charge transport property of ZGNR are closely related to the symmetry. The asymmetric ZGNRs present distinctly different transport behavior from the symmetric ones under bias voltages [7]. In addition, the perfect spin-filtering effect can be achieved in ZGNR with asymmetry edge hydrogenation by boron or nitrogen doping [32]. In experiment, the perfect ZGNR with atomically precise zigzag edges can be synthesized using the bottom-up method through surface assisted polymerization and cyclodehydrogenation of specifically designed precursor monomers [33]. And the growth of graphene nanoribbon (GNR) with smooth edge and controllable width can be achieved on the substrates of hexagonal boron nitride by using chemical vapour deposition [34].

The spin polarization closely depends on the (DOS) at the FL according to the Stoner criterion [35–37]. Meanwhile, many studies have demonstrated that the strain has a significant influence on band structure and DOS near the FL in most of 2D materials. For example, in the black phosphorene with vacancy, sufficient strain can break the bonds formed by the phosphorus atoms near the vacancy and lead to the localized magnetic moment on the under-coordinated phosphorus atoms [38]. In the graphene monolayer with 558 linear defect, the strain can enhance the localization of the defect states and flat the corresponding subbands near the FL, which greatly raises the DOS at the FL and brings the spin polarization of the defect states [37]. Thus, applying strain on ZGNRs would be an effective method for spin polarization. However, most studies focus on some single factor, such as doping, strain, external electric field or edge decoration, the study that concerns the combining effects of these elements on the electronic structure of ZGNR is lacking. Furthermore, it is inevitably to ignore the effect of strain in the reality owing to the geometric deformation induced by the substrate. In addition, the study of the coupling effect of two or more factors including strain would give some more useful suggestions in a real-world application and lead to some interesting results. Therefore, in this work, using the density functional theory, the strain effect on the magnetism and electronic structure under the transverse electric field of the pristine and the −OH and −CN groups decorated ZGNRs have been studied, and the results show that the strain greatly enhanced the magnetism of ZGNR and the half-metallicity can be preserved in the wider range of electric field.

2. Model and method

ZGNR is a structure that can be obtained by cutting graphene along the zigzag direction, and its width is usually characterized by the number of carbon chain along the periodic direction, conventionally named as n-ZGNR. Figures 1(a) and (b) present the geometric structures of the pristine ZGNR and the edge decorated ZGNR by −OH and −CN groups, respectively. The strain is applied along the periodic direction and the electric field is perpendicular to the periodic direction and parallel to the plane of ZGNR.

The geometry optimization and electronic properties are calculated by using the AtomistixToolKit (ATK) package, in

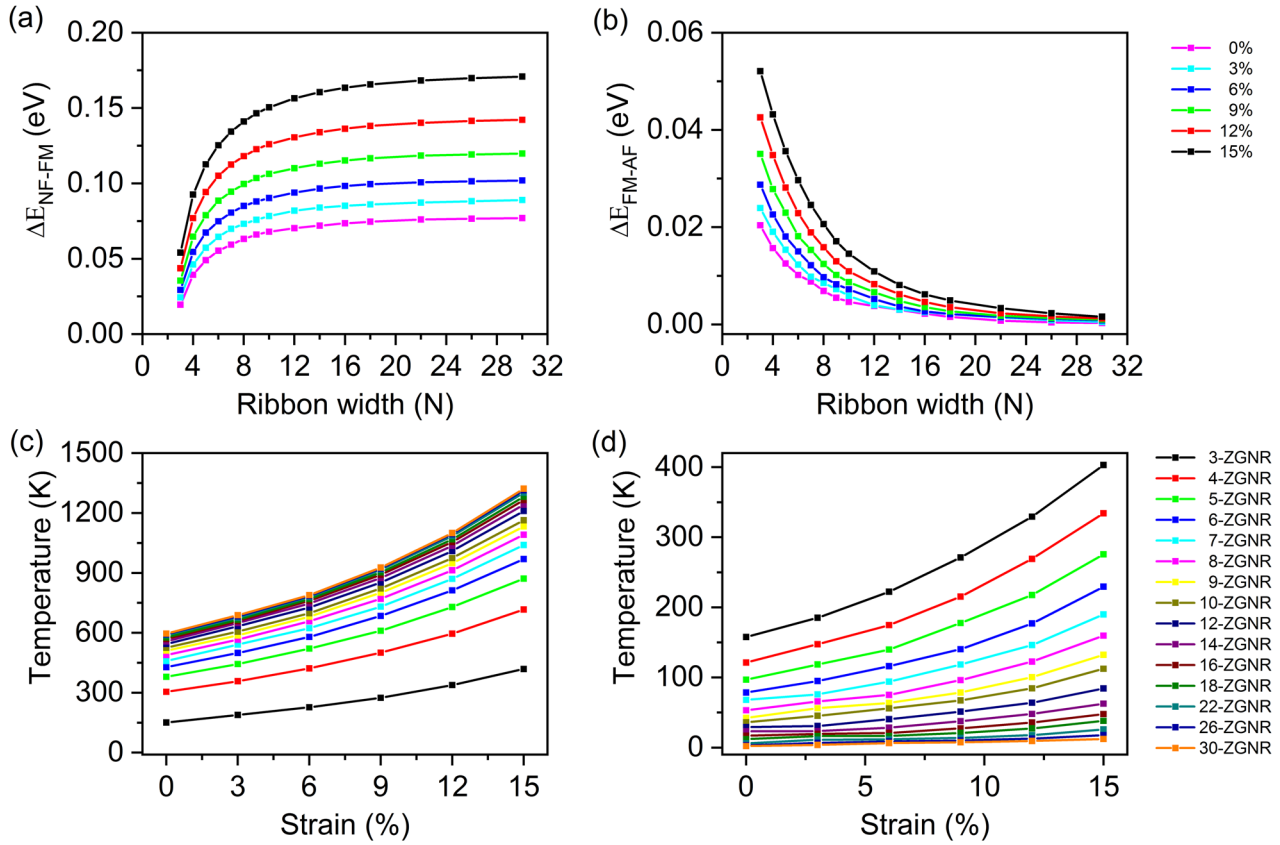

Figure 2. The total energy differences between (a) NF and FM states and (b) FM and AF as a function of the width of ZGNRS under different strains. The transformation temperatures of ZGNRs from (c) FM to NF and (d) AF to FM.

which the density functional theory (DFT) and nonequilibrium Green's function (NEGF) method [39, 40] are implemented. The Perdew–Burke–Ernzerhof (PBE) functional based on the generalized gradient approximation (GGA) is employed to describe the exchange correlation interaction [41]. The norm-conserving Troullier–Martins pseudopotentials are employed to deal with the interaction between the electrons and the ions. The spin-unrestricted ground state wave function is expanded with the duoble-zeta polarized (DZP) basis set. The cutoff energy of the real space grid is 75 Hartree and the k-point sampling is $1 \times 1 \times 101$. A vacuum layer of 20 Å is added to avoid the interaction between adjacent ribbons. The convergence criterion is that the change of total energy is less than 10^{-4} Hartree and the electron temperature is 300 K. The atom positions are optimized by using the Quasi-Newton method until the absolute value of force acting on each atom is smaller than 0.02 eV $Å^{-1}$.

In addition, the exchange correlation functional is also critical in DFT calculation. The exact exchange energy in spin-unrestricted Hartree–Fock (HF) method usually brings the artificial symmetry breaking and overestimated band gap owing to the lack of correlation term [42–43]. Reasonably consider the correlation energy can removal the artificial symmetry breaking [44]. The PBE functional simultaneously considered the exchange and correlation energy, possesses low computation cost, and can yield reasonable results in most cases, thus widely adopted by many researchers, but which tends to underestimate the band gap. Therefore, the screened exchange hybrid functional proposed by Heyd, Scuseria, and Ernzerhof (HSE06) [45–47], including one quarter of the exact exchange, has also been used to check the result especially the half-metallicity.

3. Results and discussions

The ground state of the unstrained ZGNR is antiferromagnetic. To know whether the strain can change the ground state of the ZGNR, the total energy of the strained ZGNRs with different width has been calculated in three kinds of spin-polarized configurations: nonmagnetic (NF), ferromagnetic (FM) and antiferromagnetic (AF). Figures 2(a) and (b) present the total energy differences $\Delta E_{\text{NF-FM}}$ ($\Delta E_{\text{NF-FM}} = E_{\text{tot}}(\text{NF}) - E_{\text{tot}}(\text{FM})$) and $\Delta E_{\text{FM-AF}}$ ($\Delta E_{\text{FM-AF}} = E_{\text{tot}}(\text{FM}) - E_{\text{tot}}(\text{AF})$) under different strains as a function of the width of ZGNR, respectively. Note that the $\Delta E_{\text{NF-FM}}$ gradually increases with the increase of the width of ZGNR and finally approaches a constant as shown in figure 2(a). The effect of the rising strain is evidently enhancing the value of this constant, approximately from the 75 meV under the strain of 0% to the 175 meV under the strain of 15%. For the $\Delta E_{\text{FM-AF}}$, as shown in figure 2(b), although all curves eventually decrease to zero with the increase of the width of the ribbon, the strained one drops with slower speed, which indicates that the strain can effectively slow down this tendency of decreasing. Since both $\Delta E_{\text{NF-FM}}$ and $\Delta E_{\text{FM-AF}}$ are always larger than zero, the AF state remains the ground state.

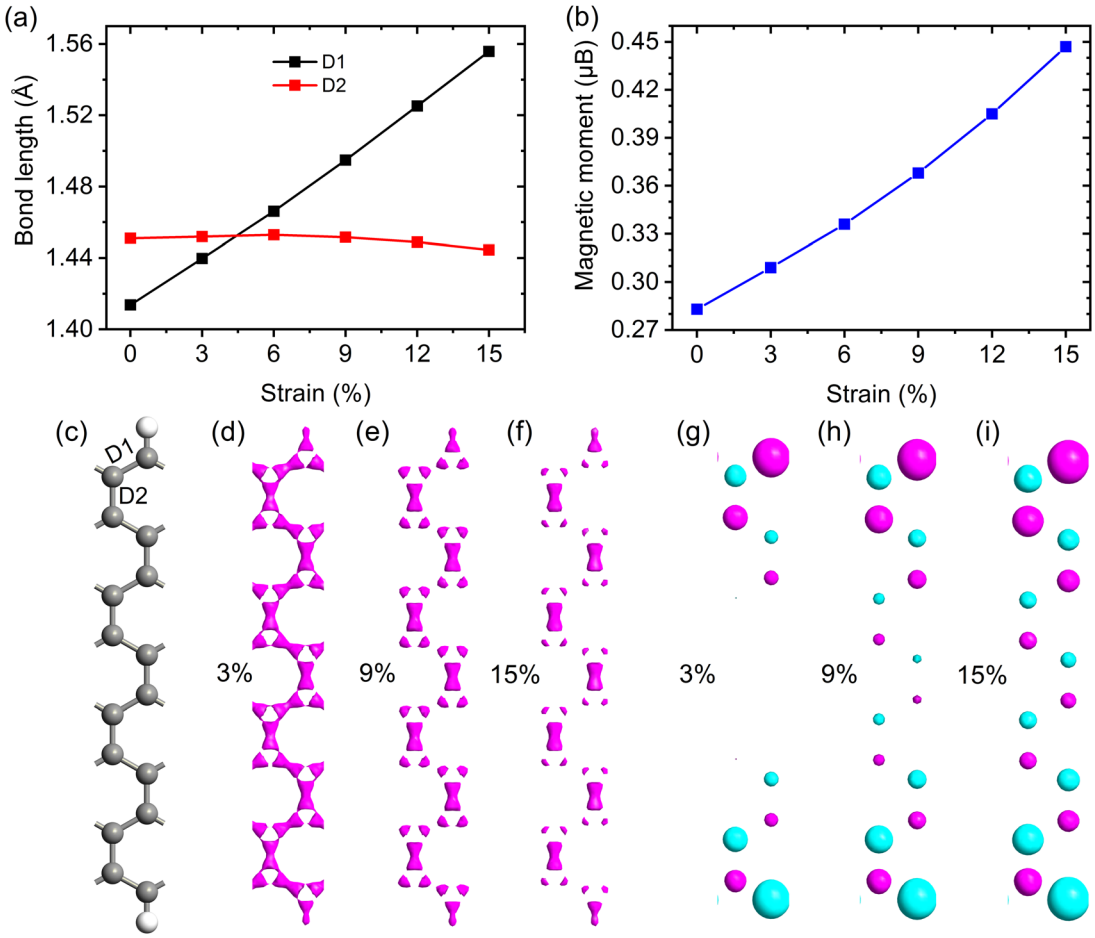

Figure 3. (a) D1 and D2 as a function of the strain. Here, as shown in (c), D1 and D2 represent the bond lengths of C–C located at the nearest edge and the next nearest edge of 8-ZGNR, respectively. (b) The magnetic moment of the carbon atom located at the nearest edge of 8-ZGNR under different strains. (c) The geometric structure of 8-ZGNR. (d)–(f) The electronic density of 8-ZGNR under the strains of 3%, 9%, 15% respectively. The isovalue is taken as 0.25 e $Å^{-3}$. (g)–(i) The spin density of 8-ZGNR under the strains of 3%, 9%, 15% respectively. The isovalue is taken as 0.005 e $Å^{-3}$.

In addition, figures 2(c) and (d) plotted the corresponding transformation temperature from FM to NF, AF to FM calculated by the mean field theory (MFT) in which $K_BT = \frac{2}{3}\Delta E$ [48, 49], where K_B and ΔE represent the Boltzmann's constant and the energy difference ($\Delta E_{NF\text{-}FM}$ or $\Delta E_{FM\text{-}AF}$) between different spin-polarized configurations, respectively. It is remarkable that the strain can effectively improve the transformation temperature between different spin-polarized configurations. And some transformations occur at higher than room temperature. For example, the transformation temperature of 4-ZGNR from the FM state to the NF state increases from 304.66 K under the strain of 0% to 716.54 K under the strain of 15%, and that from the AF state to the FM state increases from 121.38 K under the strain of 0% to 334.21 K under the strain of 15%.

To give an intuitive understanding on the strain effect, taking 8-ZGNR as an example, the influences of strain on the length of C–C bonds located at the nearest edge (D1) and the next nearest edge (D2) have been plotted in figure 3(a). D1 is very sensitive to the strain and almost linearly increases with the increase of the external strain. While D2 is not susceptible to the strain and barely changes in the whole strain range. The main reason is that the strain is along the zigzag direction and perpendicular to the C–C bond corresponding to D2, thus there is little influence on D2 while linearly stretches the D1.

Figure 3(b) presents the effect of strain on the magnetism of the carbon atom located at the edge of the 8-ZGNR. It is obvious that the magnetic moment is approximately a linear function of the strain, which indicates that the strain can effectively improve the magnetism moment. To intuitively exhibit the effect of strain on magnetism, we plotted the electron density and the spin density under the strains of 3%, 9% and 15%. It is found from figures 3(d)–(f), the electrons gradually concentrate on the C–C bond perpendicular to the periodic direction with the rising strain due to a large variation of the D1 bond. At the same time, as shown in figures 3(d)–(f), the spin density is delocalized in the nanoribbon with the increasing strain.

Moreover, the combined effect of the strain and the electric field on the gap has been considered. The the spin-dependent gaps as a function of the electric field under different strains are plotted in figures 4(a) and (b), respectively. For the spin-up states, under the strain of 0%, as shown by the magenta line in figure 4(a), we can see that the gap first decreases with the

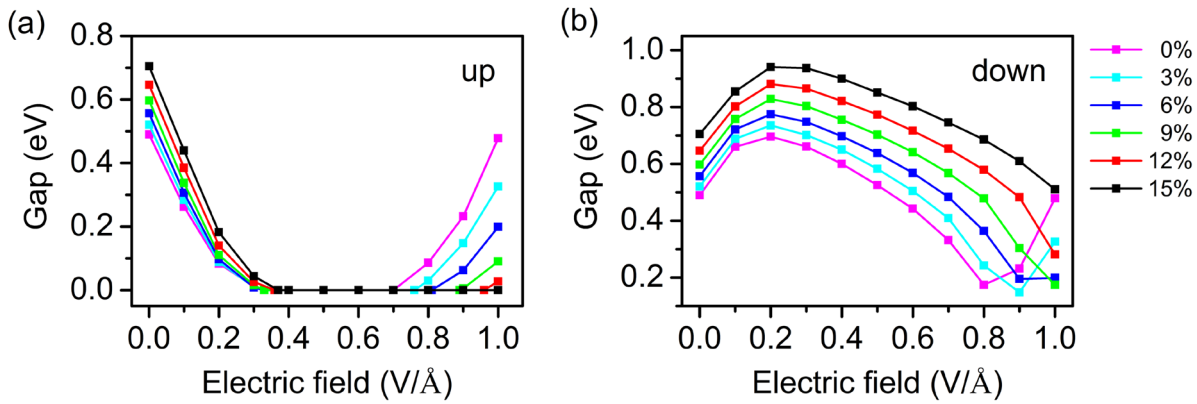

Figure 4. (a) The energy gap of spin-up and spin-down subbands for the pristine 8-ZGNR under different strains and electric fields. (b) The energy gap of spin-down subbands for the pristine 8-ZGNR under different strains and electric fields.

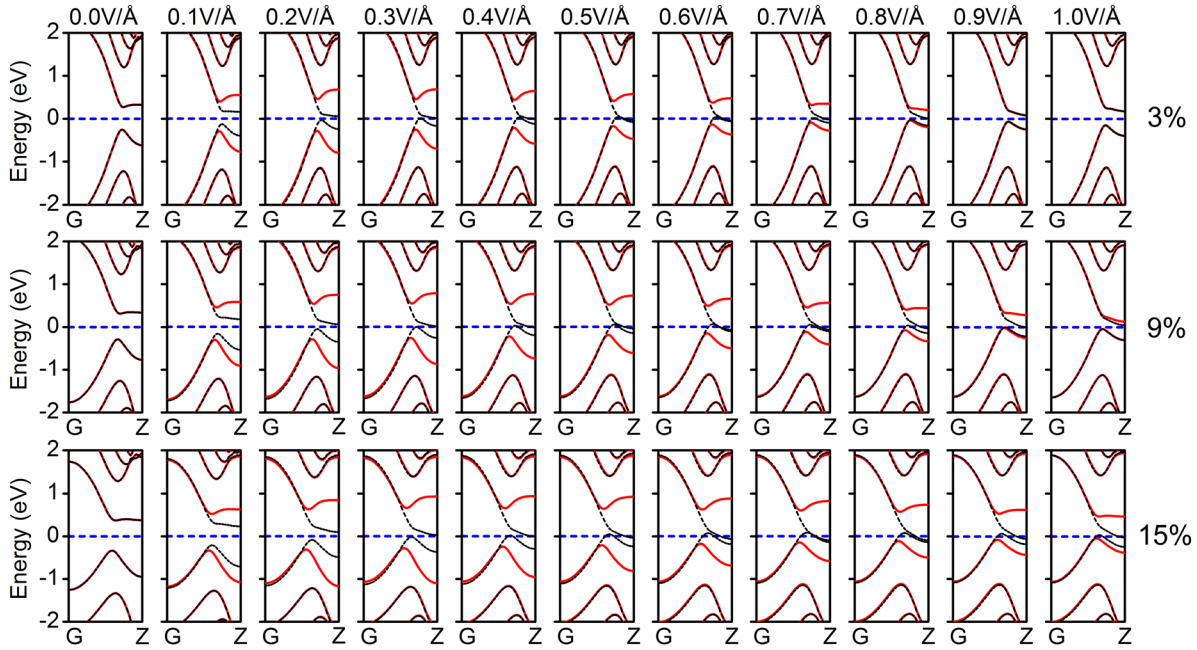

Figure 5. The band structures of the pristine 8-ZGNR under different electric fields and strains. The black short dash lines and red solid lines refer to spin-up and spin-down states, respectively. The FL is set to zero as the blue dash line shown.

increasing electric field, and then keeps zero in the range from 0.33 V Å^{-1} to 0.70 V Å^{-1}, finally increases with the rising electric field. This behavior is consistent with the previous study [50]. Under the strain of 3%, as shown by the cyan line in figure 4(a), it is clearly that the curve varies with the electric field similar to the case without strain, the main difference is that the range of the electric field in which the gap keeps zero has been broadened, from 0.33 V Å^{-1} to 0.76 V Å^{-1}. When the strain increases, as the blue, the green, the red and the black lines shown in figure 4(a), this range gradually extends with the increasing strain. At the same time, for the spin-down, as exhibited in figure 4(b), all gaps are larger than zero. These indicate that the range of the electric field to preserve the half-metallicity has been broadened by the rising strain. In addition, considering that the PBE tend to underestimate the band gap, thus we also checked the half-metallicity employing the hybrid functional HSE06 for the 8-ZGNR under the strain of 9% and the electric field of 0.8 V Å^{-1}, and we found that the calculated band structure remains the half-metallicity, which is consist with the previous studies [51, 52], this manifests our results are qualitively realiable.

For the unstrained ZGNR, the increasing transverse electric field can converts it from an antiferromagnetic semiconductor to a half metal and then to a nonmagnetic semiconductor according to the previous work [50]. Here, to explore the influence of the strain on the evolution of the electronic structure under the transverse electric field, figure 5 presents the band structures of the pristine 8-ZGNR under different electric fields and strains. By and large, the band structures of the strained ZGNR evolve as the unstrained one under the electric field [43]. For example, under the strain of 3%, as the rising of the electric field, the spin-degenerated band first splits and then displays the half-metallicity, finally exhibits the property of the spin-degenerated semiconductor, which is similar with the unstrained one. And under the stains of 9% and 15%, the band first splits and then presents the half-metallicity,

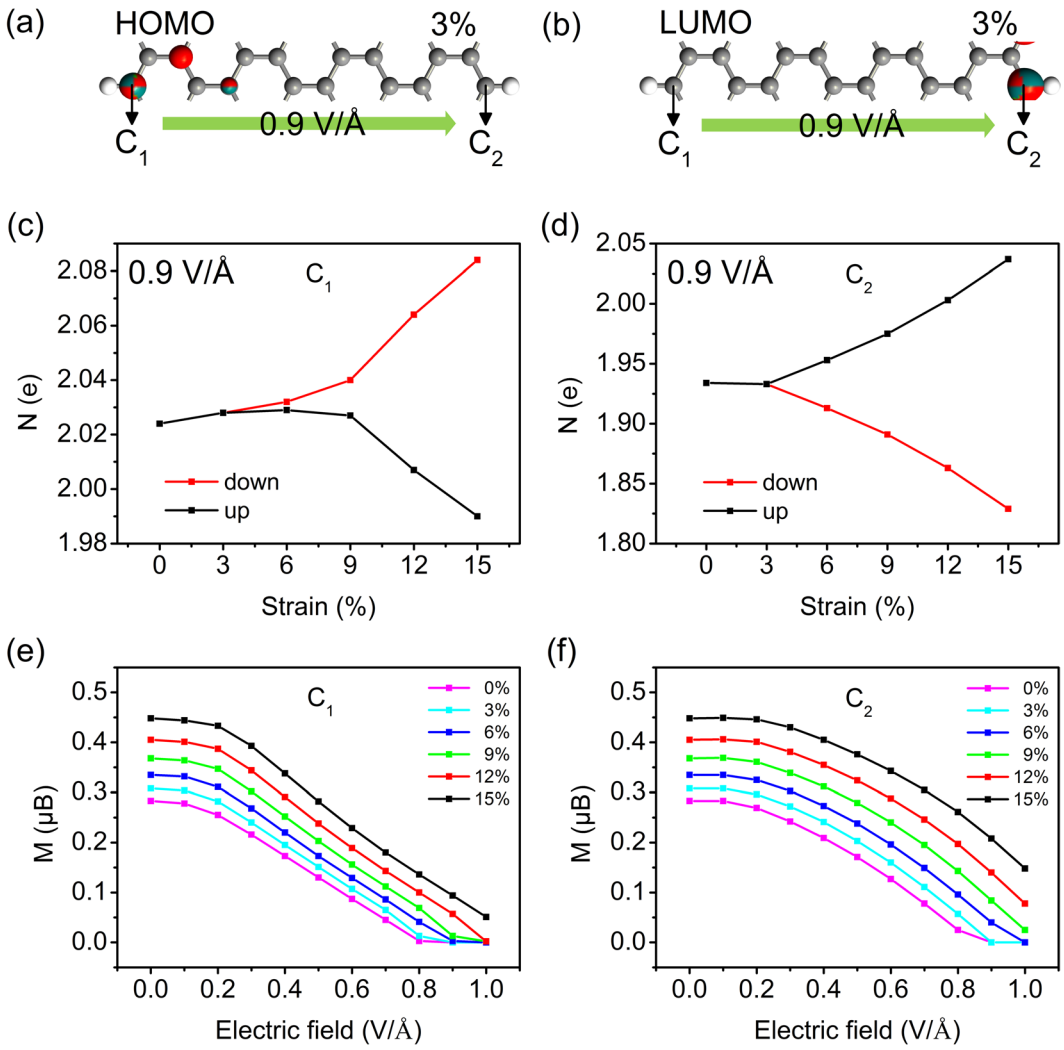

Figure 6. (a) HOMO and (b) LUMO Under the electric field of 0.9 V Å^{-1}, the Bolch state of the HOMO and the LUMO under the strain of 3%, respectively, using C_1 and C_2 denote the carbon atom located at the edge with high and low electrostatic potential, respectively. (c)–(d) The number of the spin-up and the spin-down electrons of the edge carbon atoms C_1 and C_2 as a function of strain under the electric field of 0.9 V Å^{-1}, respectively. (e)–(f) The magnetic moments of the edge carbon atoms C_1 and C_2 under different strains and electric fields, respectively.

comparing with the unstrained one, the main difference is that the transformation from a half metal to a spin-degenerated semiconductor does not occur in the range from 0 V Å^{-1} to 1.0 V Å^{-1}.

On the other hand, the influences of the strain on the band structures of ZGNR also depend on the electric field. When the electric field is smaller than 0.8 V Å^{-1}, the band structures are not sensitive to the strain. For example, without the electric field, the band structures under 3%, 9% and 15% are spin-degenerated. And under the electric field of 0.4 V Å^{-1}, the band structures always present the half-metallicity, regardless of the strains 3%, 9%, 15%. While when the electric field is larger than 0.8 V Å^{-1}, the strain can effectively modulate the band structure. For example, under the electric field of 0.9 V Å^{-1}, the system evidently exhibits different properties under different strains. Under the strain of 3%, the band of 8-ZGNR is spin-degenerated, when the strain increases to 9%, the band splits with a energy gap of 0.005 eV, and when the strain approaches to 15%, the spin-up subbands cross the FL and the system converts into a half metal. Thus the strain can broaden the range of the electric field to preserve the half-metallicity.

This strain-induced transformation from the semiconductor to the half metal under 0.9 V Å^{-1} can be understood by the Hubbard model [35], based on which the energy of the spin-up and the spin-down edge states can be approximately expressed as $E_{k\uparrow} = E_k + UN_\downarrow$ and $E_{k\downarrow} = E_k + UN_\uparrow$ respectively. Here, E_k represents the energy without considering spin polarization, parameter U is the exchange integral describing the Coulomb repulsion interaction between the spin-up electron and the spin-down electron of the edge carbon atom, $N_\downarrow$ and $N_\uparrow$ represent the number of the spin-up and the spin-down electrons of the edge carbon atom, respectively. Under the electric field of 0.9 V Å^{-1}, when the strain of 3% was applied, as shown in figure 6(a), we can see that the highest occupied molecular orbital (HOMO) mainly contributed by C atom located at the edge with high electrostatic potential, using C_1 denoting this C atom. For the 8-ZGNR under the electric field of 0.9 V Å^{-1}, figure 6(c) presented the number of the spin-up

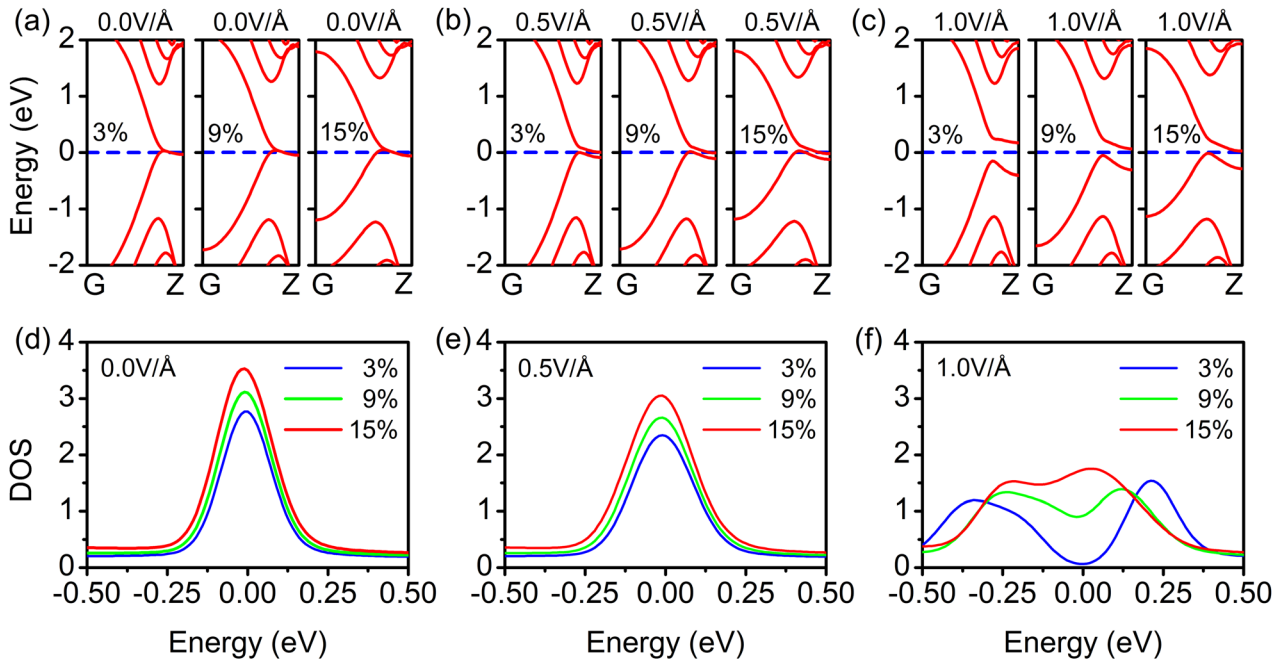

Figure 7. The band structures and the DOS under different strains and electric fields without the consideration of spin-polarization. (a)–(c) The band structures of the 8-ZGNR under the strains of 3%, 9% and 15%, corresponding to the electric fields of 0.0 V Å^{-1}, 0.5 V Å^{-1}, 1.0 V Å^{-1} respectively. (d)–(e) The DOS of the 8-ZGNR under the strains of 3%, 9% and 15%, corresponding to the electric fields of 0.0 V Å^{-1}, 0.5 V Å^{-1}, 1.0 V Å^{-1} respectively.

Table 1. Calculated ranges of electric field to preserve the half-metallicity for the pristine and the O–H/C–N-functionalized 8-ZGNR under different strains, labeled as E_{R1} and E_{R2} respectively.

Strain (%)	E_{R1} (V Å^{-1})		E_{R2} (V Å^{-1})	
	Positive	Negative	Positive	Negative
0	0.33–0.70	−0.33 to −0.70	0.45–0.72	−0.15 to −0.45
3	0.33–0.76	−0.33 to −0.76	0.46–0.77	−0.16 to −0.50
6	0.33–0.81	−0.33 to −0.81	0.46–0.83	−0.16 to −0.55
9	0.33–0.89	−0.33 to −0.89	0.47–0.90	−0.17 to −0.60
12	0.36–0.96	−0.36 to −0.96	0.49–0.96	−0.18 to −0.66
15	0.37–1.00	−0.37 to −1.05	0.53–1.05	−0.19 to −0.74

and the spin-down electrons of the C_1 atom as a function of strain under the electric field of 0.9 V Å^{-1}. It can be noted that the number of the spin-down electrons gradually increases with the rising strain, while that of the spin-up gradually decreases within the range from 6% to 15%. Thus under the electric field of 0.9 V Å^{-1}, as the increase of the strain, the spin-up HOMO shift upward owing to $E_{k\uparrow} = E_k + UN_{\downarrow}$, while the spin-down HOMO shift downward owing to $E_{k\downarrow} = E_k + UN_{\uparrow}$.

For the lowest unoccupied molecular orbital (LUMO), as shown in figure 6(b), it mainly contributed by C atom located at the edge with low electrostatic potential, using C_2 denoting this C atom. Figure 6(d) presented the number of the spin-up and the spin-down electrons of the C_2 atom as a function of strain under the electric field of 0.9 V Å^{-1}. It can be noted that the number of the spin-down electrons gradually decreases with the rising strain, while that of the spin-up gradually increases with the increasing strain. Therefore, under the electric field of 0.9 V Å^{-1}, as the increasing of the strain, the spin-up LUMO shift downward owing to $E_{k\uparrow} = E_k + UN_{\downarrow}$, while the spin-down LUMO shift upward owing to $E_{k\downarrow} = E_k + UN_{\uparrow}$. Therefore, from above analysis, the strain-induced transformation from the semiconductor to the half metal mainly originates from the strain-induced improvement of the spin polarization of the C_1 and the C_2 atoms. In addition, figures 6(e) and (f) present the magnetic moment of the C_1 and the C_2 atoms respectively, which monotonously decreases with the increasing electric field while gradually increases with the rising of the strain. This further indicates that the strain can enhance the spin polarization of the edge carbon atoms.

To further understand why the strain can raise the spin polarization of the edge carbon atoms in 8-ZGNR, the band structures and the DOS without considering spin-polarization under different strains and electric fields have been shown in figure 7. Under the zero electric field, as shown in figure 7(a), it is obvious that the flat part of the edge subbands near the FL is extended by the increasing strain. Accordingly, as shown in figure 7(d), the peak of the DOS at the FL gradually increases with the rising of the strain. When the electric field was applied, the states contributed by different edge move

apart each other owning the different electrostatic potential of the two edges introduced by the electric field, which accordingly brings the decrease of the DOS at the FL. For example, under the electric field of 0.5 V Å^{-1}, as shown in figure 7(b), there is a very small gap between the two subands, and the corresponding DOS has also been presented in figure 7(e), comparing with that under zero electric field as shown in figure 7(d), we can find that the DOS at the FL decreased for the same strain. Under the electric field of 1.0 V Å^{-1}, as shown in figure 7(c), there is an obvious gap between the two subands can be observed, which is corresponding to the DOS greatly decrease as exhibited in figure 7(f). In short, the strain enhances the DOS at the FL while the electric field reduces it. And thus according to the Stoner criterion, spin polarization is closely dependent on the DOS of local states at FL, the higher peak of DOS, the more beneficial to spin-splitting. So it can be concluded that the strain can enhance the spin-splitting of ZGNR, while the electric field can weaken this effect.

In addition to the effects of the strain and electric field, another important factor in turning the electronic structure and spin polarization is edge decoration. Here, the strain effect on the O-H/C-N-decorated 8-ZGNR has also been calculated. Table 1 lists the ranges of electric field to preserve the half-metallicity for the pristine and the O–H/C–N-functionalized 8-ZGNR under different strains. Obviously, the external strain also extends the range of electric field to preserve the half-metallicity. The mechanism is same as in the pristine 8-ZGNR. In addition, the O–H/C–N-functionalized 8-ZGNR possesses lower critical electric field to realize half-metallicity comparing with the pristine 8-ZGNR. The reason is that the functional groups result in the shift of edge subbands, which bring the similar effect as the transverse electric field, thus a smaller electric field can induce the half-metallicity [50]. These results manifest that one can simultaneously extend the range of electric field and lower the critical electric field by combining external strain and edge decoration to improve the half-metallicity.

4. Conclusions

In conclusion, the influences of strain on the spin-dependent electronic structures of the ZGNR under transverse electric field have been calculated. The results indicated that instead of changing the ground state of ZGNR, the tensile strain makes the antiferromagnetic state becomes more stable. Furthermore, when the electric field is larger than 0.8 V Å^{-1}, the strain can transform the 8-ZGNR from a semiconductor to a half metal, which broadened the range of the electric field to preserve the half-metallicity. In addition, the coupling effect of external strain, transverse electric field and O–H/C–N decoration for 8-ZGNR has been studied. Moreover, the strain can localize the edge states and then enhance the spin polarization, but which fail to effectively move the edge states. On the contrary, the transverse electric field can effectively shift the edge states, but which tend to reduce the spin polarization of the ZGNRs. The O–H/C–N decoration possesses similar effect as the electric field and can lower the critical electric field to realize half-metallicity. Combining the three factors, the range of electric field to realize half-metallicity can be widened by applying strain due to the enhanced spin polarization of edge states, at the same time, the critical electric field can be lowered by the O–H/C–N decoration.

Acknowledgments

We gratefully acknowledge support by the National Natural Science Foundation of China (Grant No. 21673296), and the Natural Science Foundation of Hunan Province (Grant No. 2018JJ2481) and Jiangxi Province (Grant No. 20171BAB211010).

ORCID iDs

Mengqiu Long https://orcid.org/0000-0003-4184-9177

References

[1] Novoselov K S, Geim A K, Morozov S V, Jiang D, Zhang Y, Dubonos S V, Grigorieva I V and Firsov A A 2004 *Science* **306** 666–9
[2] Bostwick A, Ohta T, Seyller T, Horn K and Rotenberg E 2007 *Nat. Phys.* **3** 36
[3] Zhang Y, Tan Y-W, Stormer H L and Kim P 2005 *Nature* **438** 201
[4] Lee C, Wei X, Kysar J W and Hone J 2008 *Science* **321** 385
[5] Long M-Q, Tang L, Wang D, Wang L and Shuai Z 2009 *J. Am. Chem. Soc.* **131** 17728–9
[6] Balandin A A, Ghosh S, Bao W, Calizo I, Teweldebrhan D, Miao F and Lau C N 2008 *Nano Lett.* **8** 902–7
[7] Li Z, Qian H, Wu J, Gu B-L and Duan W 2008 *Phys. Rev. Lett.* **100** 206802
[8] Vogt P, De Padova P, Quaresima C, Avila J, Frantzeskakis E, Asensio M C, Resta A, Ealet B and Le Lay G 2012 *Phys. Rev. Lett.* **108** 155501
[9] Li G X, Li Y L, Liu H B, Guo Y B, Li Y J and Zhu D B 2010 *Chem. Commun.* **46** 3256–8
[10] Li M, Zhang D, Gao Y, Cao C and Long M 2017 *Org. Electron.* **44** 168–75
[11] Peng D, Zhang X, Li X, Wu D and Long M 2018 *J. Appl. Phys.* **124** 184303
[12] Song L *et al* 2010 *Nano Lett.* **10** 3209–15
[13] Dong Y, Zeng B, Xiao J, Zhang X, Li D, Li M, He J and Long M 2018 *J. Phys.: Condes. Matter* **30** 125302
[14] Din H U, Idrees M, Albar A, Shafiq M, Ahmad I, Nguyen C V and Amin B 2019 *Phys. Rev.* B **100** 165425
[15] Zhang C-X, Li Q, Tang L-M, Yang K, Xiao J, Chen K-Q and Deng H-X 2019 *J. Mater. Chem.* C **7** 6052–8
[16] Kopf M, Eckstein N, Pfister D, Grotz C, Kruger I, Greiwe M, Hansen T, Kohlmann H and Nilges T 2014 *J. Cryst. Growth* **405** 6–10
[17] Mannix A J *et al* 2015 *Science* **350** 1513
[18] Xie Z *et al* 2018 *Adv. Funct. Mater.* **28** 1705833
[19] Tang L-P, Li Q-Z, Zhang C-X, Ning F, Zhou W-X, Tang L-M and Chen K-Q 2019 *J. Magn. Magn. Mater.* **488** 165354
[20] Yi X, Long M, Liu A, Li M and Xu H 2018 *J. Appl. Phys.* **123** 204303
[21] Son Y-W, Cohen M L and Louie S G 2006 *Phys. Rev. Lett.* **97** 216803
[22] Zhang D, Long M, Zhang X, Cui L, Li X and Xu H 2017 *J. Appl. Phys.* **121** 093903

[23] Sforzini J *et al* 2016 *Phys. Rev. Lett.* **116** 126805
[24] Pham K D, Hieu N N, Phuc H V, Fedorov I A, Duque C A, Amin B and Nguyen C V 2018 *Appl. Phys. Lett.* **113** 171605
[25] Phuc H V, Hieu N N, Hoi B D and Nguyen C V 2018 *Phys. Chem. Chem. Phys.* **20** 17899–908
[26] Tang H-K, Laksono E, Rodrigues J N B, Sengupta P, Assaad F F and Adam S 2015 *Phys. Rev. Lett.* **115** 186602
[27] Yang G, Li B, Zhang W, Ye M and Ma T 2017 *J. Phys.: Condes. Matter* **29** 365601
[28] Mak K F, Lui C H, Shan J and Heinz T F 2009 *Phys. Rev. Lett.* **102** 256405
[29] Zeng B, Dong Y, Yi Y, Li D, Zhang S and Long M 2019 *J. Phys.: Condes. Matter* **31** 165502
[30] Magda G Z, Jin X, Hagymási I, Vancsó P, Osváth Z, Nemes-Incze P, Hwang C, Biró L P and Tapasztó L 2014 *Nature* **514** 608–11
[31] Son Y W, Cohen M L and Louie S G 2006 *Nature* **444** 347–9
[32] Kang J, Wu F and Li J 2011 *Appl. Phys. Lett.* **98** 083109
[33] Ruffieux P *et al* 2016 *Nature* **531** 489
[34] Chen L *et al* 2017 *Nat. Commun.* **8** 14703
[35] Hubbard J and Flowers Brian H 1963 *Proc. R. Soc.* A **276** 238–57
[36] Seo D-K and Kim S-H 2008 *J. Comput. Chem.* **29** 2172–6
[37] Alexandre S S and Nunes R W 2017 *Phys. Rev.* B **96** 075445
[38] Chintalapati S, Shen L, Xiong Q and Feng Y P 2015 *Appl. Phys. Lett.* **107** 072401
[39] Brandbyge M, Mozos J-L, Ordejón P, Taylor J and Stokbro K 2002 *Phys. Rev.* B **65** 165401
[40] Taylor J, Guo H and Wang J 2001 *Phys. Rev.* B **63** 245407
[41] Perdew J P, Burke K and Ernzerhof M 1996 *Phys. Rev. Lett.* **77** 3865–8
[42] Sherrill C D, Lee M S and Head-Gordon M 1999 *Chem. Phys. Lett.* **302** 425–30
[43] Kim Y-S, Hummer K and Kresse G 2009 *Phys. Rev.* B **80** 035203
[44] Fuchs M, Niquet Y M, Gonze X and Burke K 2005 *J. Chem. Phys.* **122** 094116
[45] Heyd J, Scuseria G E and Ernzerhof M 2003 *J. Chem. Phys.* **118** 8207–15
[46] Paier J, Marsman M, Hummer K, Kresse G, Gerber I C and Ángyán J G 2006 *J. Chem. Phys.* **124** 154709
[47] Vydrov O A, Heyd J, Krukau A V and Scuseria G E 2006 *J. Chem. Phys.* **125** 074106
[48] Anisimov V I, Aryasetiawan F and Lichtenstein A I 1997 *J. Phys.: Condes. Matter* **9** 767–808
[49] Choudhuri I, Garg P and Pathak B 2016 *J. Mater. Chem.* C **4** 8253–62
[50] Rezapour M R, Yun J, Lee G and Kim K S 2016 *J. Phys. Chem. Lett.* **7** 5049–55
[51] Hod O, Barone V and Scuseria G E 2008 *Phys. Rev.* B **77** 035411
[52] Kan E-J, Li Z, Yang J and Hou J G 2007 *Appl. Phys. Lett.* **91** 243116